Defective Glucose Metabolism in Polycystic Kidney Disease Identifies A Novel Therapeutic Paradigm

Rowe I., Chiaravalli M., Mannella V., Ulisse V., Quilici G., Pema M., Song W. X., Xu H., Mari S., Qian F., Pei Y., Musco G., and Boletta A.

Figure S1

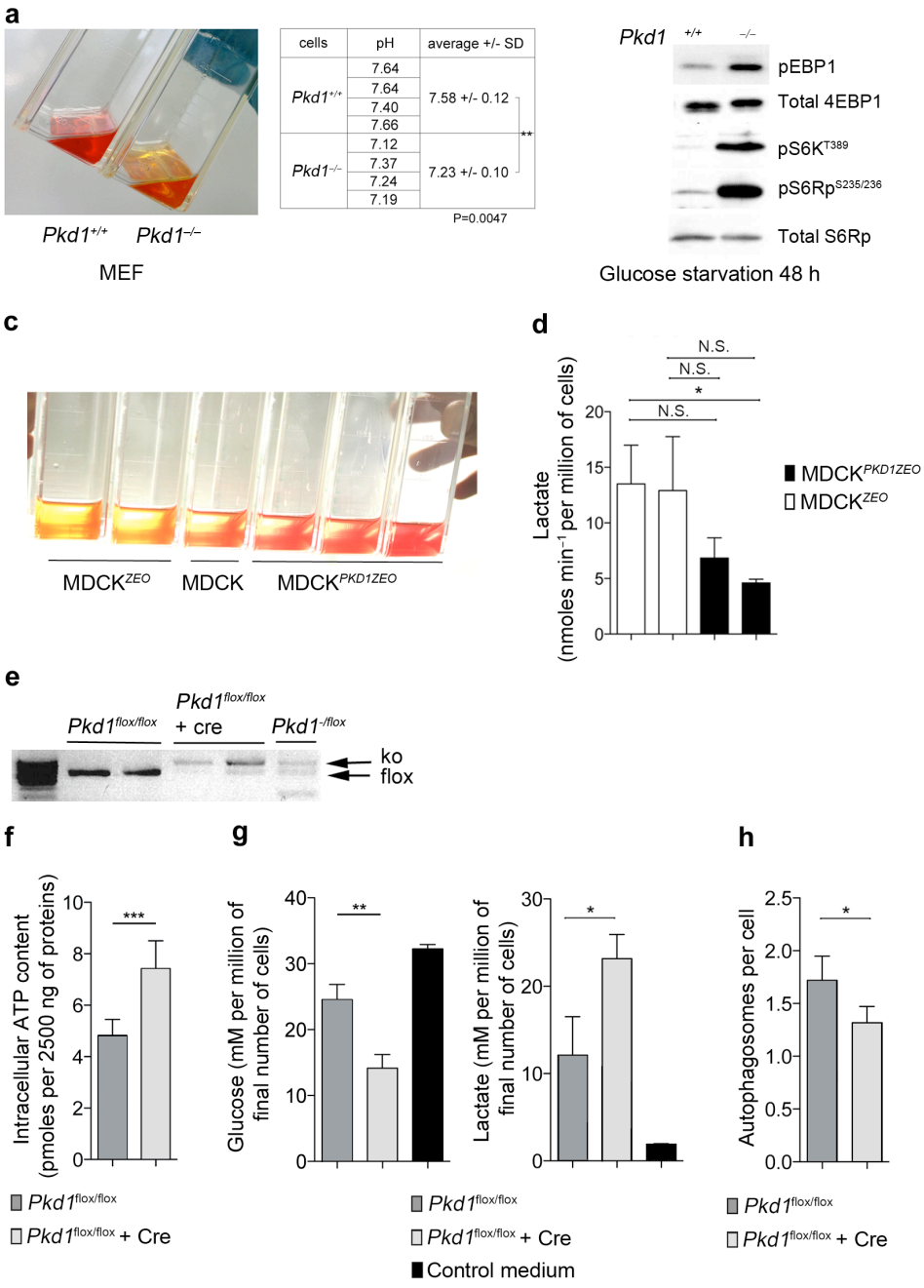

Figure S1: ***Pkd1* absence correlates with a more acid culture medium.**
a. Left. The culture medium from *Pkd1*$^{-/-}$ MEFs was more yellow than the me dium of *Pkd1*$^{+/+}$ MEFs suggesting an increased acidification. **Right.** Measurement of the pH of t he medium derived from *Pkd1*$^{+/+}$ and *Pkd1*$^{-/-}$ MEFs revealed that the latter have indeed a significantly lower pH. **b**. Downsteam targets of the mTOR pathway are up-regulated in *Pkd1*$^{-/-}$ MEFs cells after 48 h of glucose starvation. **c.** The cu lture medium of MDCK cells overexpressing the *hPKD1* gene appears less acid than the medium of control cells. **d.** Measurement of the level of lactate in the extracellular medium indicates a reduced production of la ctate in MDCK cells over-expressing the *PKD1* gene. **e.** PCR analysis of the genomic DNA derived from *Pkd1*$^{flox/flox}$ cells treated in the presence or absence of a TatCre protein revealed that the last achieve a high degree of *Pkd1* inactivation. **f.** Intracellular ATP content is increased in Cre-treated *Pkd1*$^{flox/flox}$ cells compared to untreated cells. **g.** Quantitative analysis of NMR spectra revealed decreased glucose concentration in the medium derived from *Pkd1*$^{flox/flox}$:Cre compared to that derived from *Pkd1*$^{flox/flox}$ cells and increased lactate concentration in the medium derived from *Pkd1*$^{flox/flox}$:Cre as compared to *Pkd1*$^{flox/flox}$ cells. **h.** Quantification of autophagosomes per cells evaluated by EM upon induction of autophagy with rapamycin treatment (50 nM). N.S.: $P \geq 0.05$; *: $P < 0.05$; **: $P < 0.01$; ***:$P < 0.001$; Means +/– SD are shown. T-test was performed in **d**, **f** and **g**.

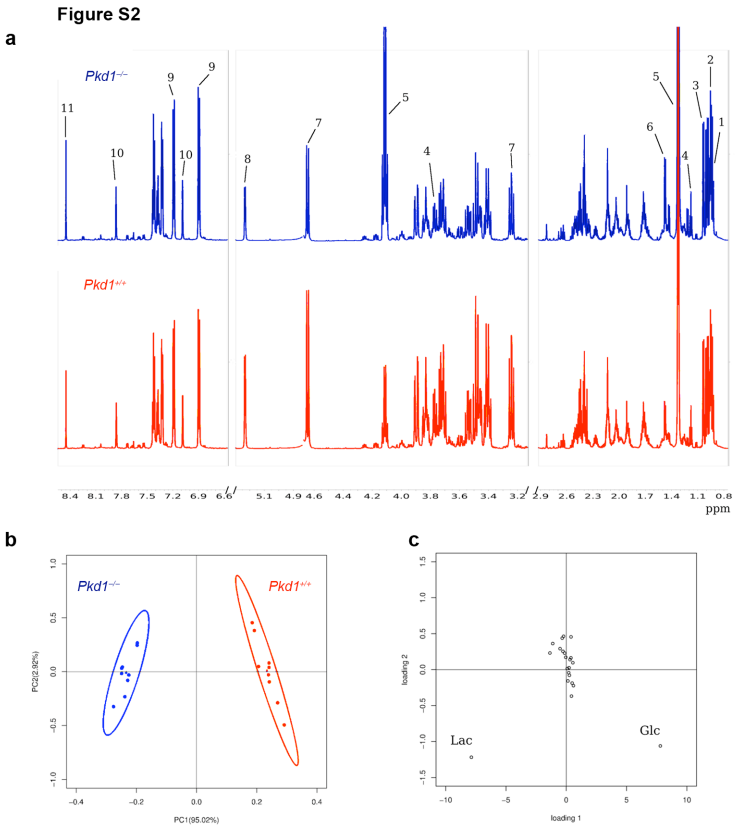

Figure S2: Metabolic profiling of the extrac ellular medium shows increased glucose uptake and lactate production of *the Pkd1*$^{-/-}$ MEFs.

Metabolic profiling of the extracellular medium conditioned with *Pkd1*$^{-/-}$ and Pkd1$^{+/+}$ MEFs. **a.** Representative 1D-1H CPMG NMR spectra of *Pkd1*$^{-/-}$ and *Pkd1*$^{+/+}$ MEFs conditioned medium with assignments: 1=Leucine; 2=Valine; 3=Isoleucine; 4=Ethanol; 5=Lactate; 6=Alanine; 7=β-glucose; 8=α-glucose; 9=Tyrosine; 10=Histidine; 11=Formic acid. Assignment details are listed in Supplementary Table 1. **b.** Principal component analysis (PCA) score plot and **c.** loading plot. PCA allows to cluster the spectra into medium conditioned with *Pkd1*$^{-/-}$ MEFs (blue) and with *Pkd1*$^{+/+}$ MEF (red) Ellipsoids around groups correspond to the 95% confidence interval. The loading plot of the first and the second principal component (PC1 and PC2) indicates that glucose and lactate, are the main metabolites distinguishing the exometabolome of *Pkd1*$^{-/-}$ MEFs from the one of *Pkd1*$^{+/+}$ MEFs.

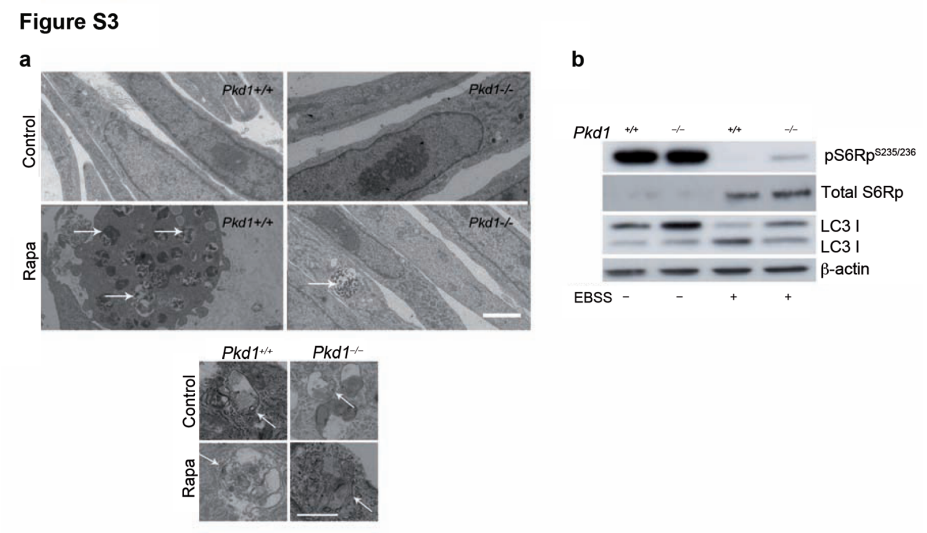

Figure S3: Analysis of Autophagy by EM.

a. Electron microscopy images show autophagosomes in *Pkd1*$^{+/+}$ and *Pkd1*$^{-/-}$ MEF cells treated in the presence or absence of rapamycin 50nM. In the bottom panel are represented zooms of autophagosomes where the typical double membrane of autophagosmes is indicated with an arrow. **b**. *Pkd1*$^{+/+}$ and *Pkd1*$^{-/-}$ MEF were cultured in the presence of EBSS for 3 h followed by western blot analysis using anti-LC3 antibodies, revealing defective autophagy in *Pkd1*$^{-/-}$ cells.

In **a**, the bar represents 2 μm in the top panel 1 μm in the above panel

Figure S4

a

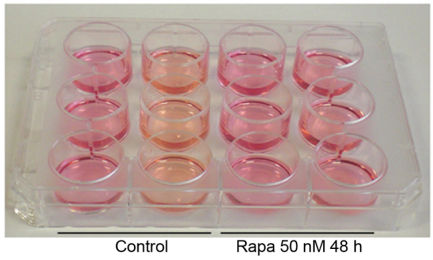

b

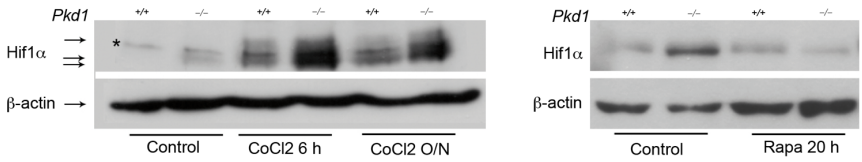

Figure S4: mTORC1-dependent acidification and HIF1alpha activation in *Pkd1*$^{-/-}$ Cells.
a. Rapamycin treatment fr 48 h at 50 nM rescues the acidification of the medium from *Pkd1*$^{-/-}$ MEFs. **b**. Western of H if1-α of *Pkd1*$^{+/+}$ and *Pkd1*$^{-/-}$ cells showing up-regulation of Hif1-α in *Pkd1*$^{-/-}$ MEF compared to i ncreased by treatment with $CoCl_2$ at 1 mM for 6 h or over night. Treatment with rapapamycin 20 nM for 20 h does rescue the Hif1-α up-regulation in *Pkd1*$^{-/-}$ MEF.

Figure S5

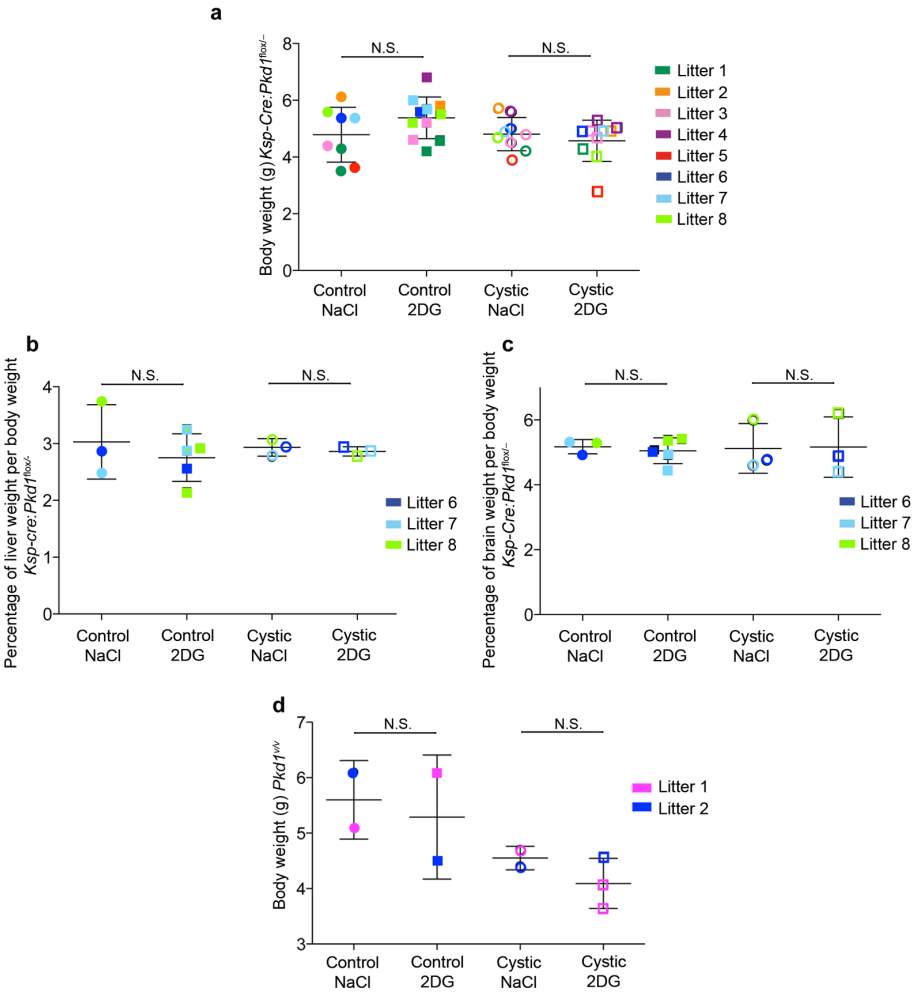

Figure S5: 2DG treatment does not alter the global physiology

a. 2DG treatment did not alter the body weight from mutant mice (*Ksp-Cre:Pkd1*$^{flox/-}$) or wt mice (*Ksp-Cre:*Pkd1$^{flox/+}$). **b**. organs weight like livers (**b**) and brains (**c**) normalised by body weight did not showed effect of 2DG. **d.** Body weight from mutant mice *Pkd1*$^{v/v}$ or control mice after treatment with 2DG or vehicle.

N.S.: $P \geq 0.05$. Mann-Whitney test was performed.

metabolite	[a]peak used for quantification (ppm)	[b] *Pkd1*$^{+/+}$ (mM·10^{-6}/cell)	[b] *Pkd1*$^{-/-}$ (mM·10^{-6}/cell)	[c] *Pkd1*$^{+/+}$ $_{rel}$	[c] *Pkd1*$^{-/-}$ $_{rel}$	[d]t-test (*Pkd1*$^{+/+}$/*Pkd1*$^{-/-}$)
glucose	5.24-5.23 [e](d) alpha 3.26-3.23 [e] (t) beta	13.54 (0.20)	6.27 (0.08)	-0.24	-0.59	***
lactate	4.13-4.10 [e](q)	5.31 (0.10)	12.80 (0.25)	3.61	12.25	***
pyruvate	2.37 [e](s)	0.0998 (0.0019)	0.033 (0.0002)	25.47	9.39	***
succinate	2.40 [e](s)	0.2628 (0.0021)	0.2252 (0.0078)	-0.03	-0.02	ns
choline	3.20 [e](s)	0.0108 (0.0002)	0.0095 (0.0002)	-0.67	-0.63	**
formate	8.45 [e](s)	0.0947 (0.0018)	0.0901 (0.0006)	2.87	3.41	***
ethanol	3.68-3.66 [e](q)	0.440 (0.003)	0.399 (0.013)	-0.16	-0.11	ns
alanine	1.48-1.47 [e](d)	0.23 (0.01)	0.279 (0.002)	0.39	0.98	***
arginine	1.67-1.60 [e](m)	0.325 (0.003)	0.251 (0.009)	-0.29	-0.21	ns
glutamate	2.36-2.33 [e](m)	0.132 (0.002)	0.246 (0.007)	0.11	1.52	***
glutamine	2.21-2.06 [e](m)	1.900 (0.020)	1.800 (0.050)	-0.57	-0.60	ns
glycine	3.56 [e](s)	0.384 (0.007)	0.277 (0.005)	0.28	0.07	***
histidine	7.09 [e](s)	0.155 (0.002)	0.122 (0.003)	-0.14	-0.19	ns
isoleucine	1.01-1.00 [e](d) 0.95-0.92 [e](t)	0.474 (0.003)	0.358 (0.006)	-0.19	-0.20	ns
leucine	0.97-0.95 [e](t)	0.386 (0.003)	0.319 (0.012)	-0.28	-0.29	ns
lysine	3.07-3.04 [e](m)	0.500 (0.002)	0.428 (0.006)	-0.14	-0.14	ns
methionine	2.65-2.63 [e](t)	0.1018 (0.0005)	0.0902 (0.0012)	0.47	0.57	ns
phenylalanine	7.44-7.43-7.41 [e](m)	0.281 (0.002)	0.225 (0.001)	-0.16	-0.16	ns
threonine	3.59-3.58 [e](t)	0.700 (0.009)	0.583 (0.004)	-0.08	-0.11	ns
tryptophan	7.74-7.72 [e](d)	0.064 (0.003)	0.059 (0.002)	-0.13	-0.03	ns
tyrosine	7.20-7.18 [e](m or d)	0.286 (0.002)	0.220 (0.002)	-0.58	-0.58	ns
valine	1.04-1.03 [e](d) 0.99-0.98 [e](d)	0.435 (0.005)	0.348 (0.009)	-0.20	-0.21	ns

a. Peaks were referenced to DSS peak at 0.00ppm. Spectra were deconvolved with GSD (see Materials and Methods). More than one region per metabolite was chosen for quantification. Each area was calculated and then divided by the number of protons contributing to the integrated peaks. For glucose the anomeric proton was analysed considering the sum of the two doublets signal corresponding to alpha and beta isomers. The number of ^{1}H nuclei contributing to signals was taken into account for normalization.

b. Standard deviation are reported in parenthesis. For WT and KO conditions three biological replicas were prepared and split into three technical replicas each, which were next analysed by NMR. For control conditions (CTR) only the three technical replicas were considered. Average values and standard deviations have been calculated among the technical replicas, weighted averages (with the corresponding standard deviations) were calculated among the biological replicas. As Pkd1$^{+/+}$ and Pkd1$^{-/-}$ cells, despite being seeded in equal amounts, had different growth rates, we decided to normalize integral areas taking into account the number of cells after 24hours incubation.

c. Relative quantification of metabolites was performed using the non conditioned medium as reference (CTR) (equation 1).

$$eq.\,1 \quad Rel.Quant_i = \frac{Conc_i[X] \times Conc_i[CTR]}{Conc_i[CTR]}$$

where $Rel.Quant_i$ is the relative quantification of metabolite i; $Conc_i$ is the absolute concentration of each metabolite; X represents WT or KO condition. Negative values reflect metabolites that are up-taken from the medium, whereas positive values reflect metabolites that are released in the medium.

d. T-test was performed between WT and KO conditions (* p<0.05, **p<0.01, ***p<0.001, ns: not significant)
e. s (singlet), d (double), t (triplet), q (quartet), m (multiplet) denote peak multiplicity

Supplementary Table S1. Metabolic profiling of Pkd1$^{+/+}$ Pkd1$^{-/-}$ cells

Supplementary Legends

Supplementary Table 1 : Quantification of the metabolites in the extracellular medium from *Pkd1*$^{+/+}$ and *Pkd1*$^{-/-}$ MEFs.

Supplementary Table 2 : Glycolytic gene expression in cystic compared to minimally cystic or normal tissues.

List of the genes coding for glycolytic enzymes and their score in small cysts, medium cysts and large cyst, minimally cystic tissue and normal kidney tissue.

Supplementary Materials

NMR Sample preparation

We snap-frozed kidney samples in liquid nitrogen and stored at –80 °C until extraction. We weighted snap-frozen samples before and after lyophilization (24 h). We extracted polar metabolites from the homogenous dry tissue powder using MeOH/CHCl3 (1/1: v/v) solvent extraction strategy, as described in [Lin, C. Y.; Wu, H.; Tjeerdema, R. S.; Viant, M. R., Evaluation of metabolite extraction strategies from tissue samples using NMR metabolomics. *Metabolomics* **3**, 55-67 (2007)]. We then lyophilized polar phases for 24 h, the resulting powder was then suspended in phosphate buffer 150 mM, with addition of 100 μM DSS as internal chemical shift indicator, and sodium azide for sample preservation. Final volumes were 250 _L with 90:10 H_2O:D_2O ratio.

NMR acquisition and metabolites recognition

We acquired NMR spectra using a 600 MHz spectrometer (Bruker Avance 600 Ultra Shield TM Plus, Bruker BioSpin) equipped with a triple-resonance TCI cryoprobe with a z shielded pulsed-field gradient coil. We carried out all experiments at 298 K, spectrometer temperature was calibrated using pure methanol-*d4* sample[21]. We equilibrated sample temperature inside the spectrometer for 5 min before data acquisition. For each sample *noesygppr1d* and Carr-Purcell-Meiboom-Gill T2 filter *cpmgpr1d* Bruker pulse sequences were acquired. We applied for all experiments continuous water presaturation with a RF of 35 Hz during relaxation delay. We acquired both the *noesygppr1d* and *cpmgpr1d* experiments with 80 scans, 98K complex data points, spectral width of 20 ppm, and relaxation delay of 6 s. We used mixing time of 10 ms for the *noesygppr1d* experiment.

We multiplied Prior Fourier Transformation FIDs by an exponential function equivalent to 1.0 Hz line-broadening. We automatically phased Spectra; corrected baseline and referenced using the library Topspin AU program apk0.noe.

To facilitate metabolites identification we acquired 2D J-resolved ^{1}H NMR experiments, 2D-^{1}H-^{1}H-TOCSY (Total Correlation spectroscopy) and 2D-^{1}H-^{13}C-HSQC (Heteronuclear single quantum coherence). We acquired 2D J-resolved experiments with 12 FIDs, accumulated over 40 increments; we set spectral widths to

16.7 ppm and 78 Hz for F2 and F1, respectively; during the relaxation delay (2 s) we suppressed the water signal using presaturation. We acquired 2D-^{1}H-^{1}H-TOCSY experiments with a total of 8 FIDs for each of the 512 increments. We set spectral widths to 12 ppm for both dimensions; we suppressed water with an excitation sculpting scheme, 2 s of relaxation delay was employed. We acquired 2D-^{1}H-^{13}C-HSQC spectra with a total of 44 FIDs for each of the 300 increments. Spectral widths were set to 16 and 185 ppm for ^{1}H and ^{13}C, respectively (with offsets equal to 4.7 and 75 ppm, respectively). We suppressed the water signal using a continuous wave presaturation during the 3 s of the relaxation delay.

We identified metabolites using Metabominer [Xia, J.; Bjorndahl, T. C.; Tang, P.; Wishart, D. S., MetaboMiner--semi-automated identification of metabolites from 2D NMR spectra of complex biofluids. *BMC Bioinformatics* **9**, 507 (2008)] and CCPN Metabolomic project [The CCPN Metabolomics Project: a fast protocol for metabolite identification by 2D-NMR.Chignola F, Mari S, Stevens TJ, Fogh RH, Mannella V, Boucher W, Musco G. *Bioinformatics.* **27**, 885-6 (2011)]. We identified and quantified 22 metabolites summarized in **Supplementary Table 1**.

Metabolite quantification

The NMR profiling strategy included, peaks assignement and integration to obtain metabolites concentrations. For metabolites quantification we took advantage of the combination of (a) the algorithm called GSD (global spectrum deconvolution), available in the Mnova software package of Mestrelab [Cobas, C.; Seoane, F.; Domínguez, S.; Sykora, S.; Davies, A. N. A new approach to improving automated analysis of proton NMRSpectrosc. *Eur.* **23**, 26–30 (2010)] and (b) of a quantitative referencing strategy, known as PULCON. [Wider G., Dreier L., Measuring Protein Concentrations by NMR Spectroscopy, *JACS* **128**, 2571-2576 (2006)]. Combining the GSD algorithm with a PULCON script we deconvolved overlapping regions and performed absolute quantification also of metabolites with resonances in crowded spectral areas [Garcia-Manteiga JM, Mari S., Godejohann , Spraul M, Napoli C, Cenci S , Musco G and Sitia R, Metabolomics of B to plasma cell differentiation, *J. Proteome Res.* **10**, 4165–4176 (2011)].

Statistical Analysis of Metabolic Alterations

For statistical analysis we used the metabolites concentrations and applied the Pareto scaling of the variables prior to principal component analysis (PCA), a multivariate unsupervised statistical technique. PCA gives a global view of the systematic variation of the data while reducing its dimensionality to few principal components (PC), which account for a large amount of the total variance between the
NMR fingerprints. The final aim of PCA is to enable easy visualization of any clustering or similarity of the various samples. The results of PCA are presented in terms of score (**Supplementary Fig. 2b**) and loading plots (**Supplementary Fig. 2c**). Samples with a similar metabolic footprint tend to cluster together in score plots. Each PC is a weighted linear combination of the original descriptors and this information is shown in a loading plot.

^{13}C NMR Spectroscopy

We detected ^{13}C lactate produced after injection of ^{13}C-glucose acquiring ^{1}H-^{13}C-HSQC NMR experiments performed at 25 °C on a Bruker Avance 600 Ultra Shield TM Plus 600 MHz spectrometer equipped with triple resonance cryoprobe (TCI) and pulsed field gradients. We acquired Spectra with 1024 and 400 points in f2 and f1 respectively, 3 scans, and 16 dummy scans and a relaxation delay of 3 s was used. Spectral widths were 11 ppm and 200 ppm in f2 and f1, respectively. We suppressed water with a presaturation scheme. We processed spectra using MNova 8.0 software.
For lactate determination we integrated the peak at 1.32 ppm and 22.91 ppm, corresponding to the methyl (CH3) signal, for glucose determination we integrated the peaks corresponding to the methylene signal (C^6H2), accounting for both _- and _-glucose (3.82, 3.78, 63.41 ppm; 3.89, 3.73, 63.47 ppm).
Integrals of methyl and methylene groups were appropriately corrected for their different T1 relaxation rates and different $^{1}J_{CH}$ coupling based on the integration of the corresponding peaks obtained from 11 standard glucose and lactate solutions (1:1 stoichiometry) at different concentrations (0.5, 1, 2, 3, 4, 5, 10, 20, 40, 50 and 80 mM, respectively).
Absolute integrals ($I_{kidneys}$) were measured using the Data Analysis module of MNova. Integrals were then divided by the dry weight (DW) of the corresponding tissue ($I_{WT}=I_{kidneys\_WT}/DW_{WT;}$ $I_{KO}=I_{kidneys\_KO}/DW_{KO}$) to account for the different kidney weights

of WT and KO mice. Moreover, to account for the genetic variability within litters, for each KO mouse we normalized the integrals (I_{KO}) of glucose and lactate peaks with respect to the integral of the corresponding WT littermate (I_{WT}). We expressed results for both glucose and lactate were therefore as peaks integral ratio between KO and WT animals ($R=I_{KO}/I_{WT}$). Bar plots in (**Fig. 3e**) represent the average values and the standard deviation of five litters.

We expressed the effect of 2-deoxy-glucose (2DG) treatment (**Fig. 4g**) as ratio (R_{2DG}) between the integrals of glucose and lactate peaks of KO mice treated with 2-deoxyglucose (I_{KO_2DG}) and the integrals obtained from spectra performed on the corresponding KO littermates (I_{KO}) treated only with NaCl ($R_{2DG}= I_{KO\_2DG}/I_{KO}$). Bar plots shown in **Fig. 3e** show the average values and the standard deviation of three litters.

We followed the same procedures and normalizations for ^{13}C NMR analysis of livers.

Real Time PCR

The primers used for real time PCR analysis were the following:

beta actin

forward: 5_-AGAAAATCTGGCACCACACC-3_

reverse: 5_-CAGAGGCGTACAGGGATAGC3-3_;

AldoA1/2

forward: 5_-AGCAGAATGGCATTGTACCC-3_

reverse: 5_-AAAGTGACCCCAGTGACAGC-3_

Arbp

forward: 5_-CTTCATTGTGGGAGCAGACA-3_,

reverse: 5_-TTCTCCAGAGCTGGGTTGTT-3_;

Pdk1

forward: 5_-GGCGGCTTTGTGATTTGTAT-3_,

reverse: 5_-ACCTGAATCGGGGGATAAAC-3_;

Gapdh

forward: 5_-ACCACAGTCCATGCCATCAC-3_,

reverse: 5_-TCCACCACCCTGTTGCTGTA-3_;

Glut-1

forward: 5_-GTCGGCCTCTTTGTTAATCG-3_,

reverse: 5_-CACATACATGGGCACAAAGC-3_;

Pkm2

forward: 5_-TGTCTGGAGAAACAGCCAAG-3_,

reverse: 5_-TCCTCGAATAGCTGCAAGTG-3_;

Electron Microscopy

We fixed cell culture monolayers for 15 min at 4 °C with PAF 4% and 2.5% glutaraldehyde in 125 mM cacodylate buffer. We detached the monolayers by rubber and centrifuged at hight speed. We post-fixed the pellet (1 h) with 2% OsO4 in125 mM cacodylate buffer, washed it, dehydrated it and embedded it in Epon. We collected conventional thin sections on uncoated grids, stained themwith uranil and lead citrate and examined them in a Leo912 electron microscope.

Statistical analysis of the microarrays

We used Gene set enrichment analysis (GSEA) [Subramanian, A., Tamayo, P., Mootha, V.K., Mukherjee, S., Ebert, B.L., Gillette, M.A., Paulovich, A., Pomeroy, S.L., Golub, T.R., Lander, E.S. *et al.* Gene set enrichment analysis: a knowledge-based approach for interpreting genome-wide expression profiles. *Proc Natl Acad Sci U S A,* **102,** 15545-50 (2005)] and Significance analysis of microarrays (SAM) [Tusher, V.G., Tibshirani, R. and Chu, G. Significance analysis of microarrays applied to the ionizing radiation response. *Proc Natl Acad Sci U S A,* **98,** 5116-21 (2001)] to identify differentially expressed gene pathways and individual genes, respectively. We defined differentially expressed pathways by a NOM P-value ≤ 0.05 with a false discovery rate (FDR) ≤ 0.25, and used FDR $\leq 0.5\%$ for the individual gene comparisons.